Journal of Materials Chemistry A

Accepted Manuscript

ROYAL SOCIETY OF CHEMISTRY

www.rsc.org/materialsA

Journal of Materials Chemistry A

ARTICLE

An Efficient Hole Transport Material Based on PEDOT Dispersed with Lignosulfonate: Preparation, Characterization and Performance in Polymer Solar Cells

Received 00th January 20xx,
Accepted 00th January 20xx

DOI: 10.1039/x0xx00000x

www.rsc.org/

Yuan Li,[*a,b] and Nanlong Hong[a,b]

Inspired by the electron transfer process during oxidation of electron-rich phenol derivative structure and serious aggregation properties of lignin, we studied the hole transporting properties by hole-only devices using water soluble lignosulfonate (SL) and alky chain cross-linked lignosulfonate polymer (ASL) as active layer for the first time. SL with more phenolic group content, has higher hole mobility than ASL with less phenolic group content, which further suggested that phenolic group is conducive to the hole transporting property. The maximum value of hole mobility achieved to 3.75×10^{-6} $cm^2 V^{-1} s^{-1}$ from SL. The unexpected hole mobility provide a novel prospective for application of SL as a potential polymeric p-type semiconductor. A water soluble and solution-processable PEDOT:SL was prepared by oxidation of EDOT dispersed in SL and PEDOT:SL showed comparable performance with PCE of 5.79 % as hole-transport material in OPV with conversional PEDOT:PSS with device structure of ITO/HTM/PTB7:PC_{71}BM/Al. In principle, comparing with PSS with regular molecular structure, amorphous lignosulfonate with complex chemical structure might show worse hole transport property as dopant for PEDOT. In contrast, we found PEDOT:SL showed comparable performance with that of PEDOT:PSS. The performance of PEDOT:SL is not very dependent on the mass ratio of PEDOT in PEDOT:SL. This also confirmed our proposal and results on the hole transport property of lignosulfonate. Our results provide a promising scaffold and concept for the design and feasible synthesis of HTMs based on the interconversion between phenol and benzoquinone for organic electronics. Moreover, our result also opens a application approach of lignin in future.

Introduction

During the past decades of development of organic electronic devices including organic light emitting diodes (OLEDs),[1-4] organic solar cells (OSCs),[5-8] organic field effect transistors (OFETs)[9,10] and polymer solar cells (PSCs)[11-13], hole transport materials (HTMs), also called p-type materials, played indispensable roles and had been pursued with great interest of chemistry scientists. One of the most widely employed HTM is poly (3, 4-ethylene dioxythiophene): poly (styrene sulfonic acid) PEDOT:PSS which modify indium-tin oxide (ITO) anode with good performances,[14-16] however, it is known that PEDOT:PSS could corrode ITO at elevated temperatures due to its highly acidity.[17-19] New solution-processable HTMs are still in demand and chemistry scientists have made great effort to explore new materials.[20-26]

Considering that traditional and classical hole transport materials (PEDOT:PSS),[14-16] N,N'-di-[(1-naphthalenyl)-N,N'-diphenyl]-1,1'-biphenyl-4,4'-diamine (NPB)[27,28] and poly (vinylcarbazole) (PVK)[29] contain electron-rich building blocks thiophene-, arylamine-, and carbazole- based derivatives respectively, many work focused on the modification of these materials.[30-32] Meanwhile, most of HTMs are wide band gap p-type materials, and several inorganic materials such as V_2O_5 and MoO_3 have been reported.[33] However, solution processable organic wide band gap material is still in urgent demand.

It is well known that hole transport process during the operation of organic electronic devices is related with oxidation of electron-rich building blocks, such as typical bis(triphenylamine) and derivatives, in which the radical-cation are formed as shown in Figure 1a.[34] However, there is rarely report of HTM based on the electron-rich compounds such as phenol derivatives.

In this work, inspired by the electron transfer process during oxidation of phenol derivatives of lignin, in which radicals will be produced as shown in Figure 1b,[35] we proposed that SL might show hole transport property in organic electronic devices. The hole mobility, oxidation behavior, ESR and electrochemical property were studied carefully and discussed. Furthermore, based on the result above, we designed a novel water solution-processable hole transport material PEDOT:SL

[a] School of Chemistry and Chemical Engineering, South China University of Technology, Guangzhou, China.
[b] State Key Laboratory of Pulp and Paper Engineering, South China University of Technology, Guangzhou, China.
* Corresponding author. Email: celiy@scut.edu.cn

†Electronic Supplementary Information (ESI) available: [the results including molecular weight distribution and functional group contents of SL and ASL; FT-IR and ^{1}H-NMR of samples; conductivities of PEDOT: sample films; AFM images of PEDOT:PSS and PEDOT:ASL film after heating]. See DOI: 10.1039/x0xx00000x

which was prepared by oxidation of EDOT dispersed in SL. For comparison, PEDOT:PSS 4083 was studied as a control for the hole transport performance test.

Lignin, the second most abundant plant resource, is gaining attention of academic and industrial research interest because of the increasing crisis of oil resource.[36,37] Nowadays it has been used as an inexpensive and renewable starting material for developing new products in various aspects.[38-41] The approaches for high-value-added utilization of lignin, as the only biomass containing rich aromatic rings in nature, are still of urgent importance to be developed. It is known that native lignin shows strong absorption in ultraviolet region of sun-spectrum due to its rich aromatic rings in lignin molecules.[42] The J-aggregation behaviours of lignin and lignosulfonate have been intensively studied in our previous work as shown in Figure 1c.[43]

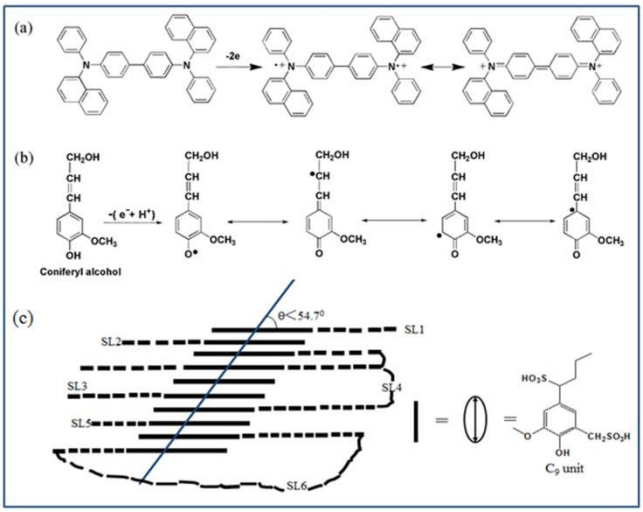

Figure 1. Resonance structures of NBP (a) and model compound of lignin during oxidation as hole transport materials (b). (c) J-aggregation behaviour of lignosulfonate (SL).

Most recently, we find that SL exhibited unexpected hole mobility because of phenolic oxidation and J-aggregation behaviour. The aggregation of SL may be potential application in semiconductor. In this context, to study the effect of phenolic group on the hole transporting property, alkyl chain was introduced to the phenolic group of sulfomethylated lignin (SL) to obtain alkyl chain cross-linked lignosulfonate-based polymer via our previous method.[44] Alkali lignin (AL), from pulping black liquor, was sulfomethylated and coupled to prepare supramolecular lignosulfonated-based amphiphilic polymer (ASL). It is noteworthy finding that ASL with ultrahigh molecular weight also showed relatively lower hole mobility comparing with that of SL and it can be explained by the lower phenolic hydroxyl group content (see Figure 1b).

Results and discussion

Supramolecular lignosulfonated-based polymer (ASL) was synthesized via sulfomethylation and alkyl chain coupling polymerization of AL. The synthetic route of ASL is shown in Figure S1. The molecular weight (Mw) and fundamental structural properties of ASL were characterized by gel-permeation chromatography (GPC), fourier transform infrared spectroscopy (FT-IR) and ^{1}H-NMR spectroscopy, respectively. As shown in Figure S1, noteworthy increase of Mw has been made through polymerization of sulfomethylated lignin (SL) using $C_6H_{12}Br_2$ reagent.

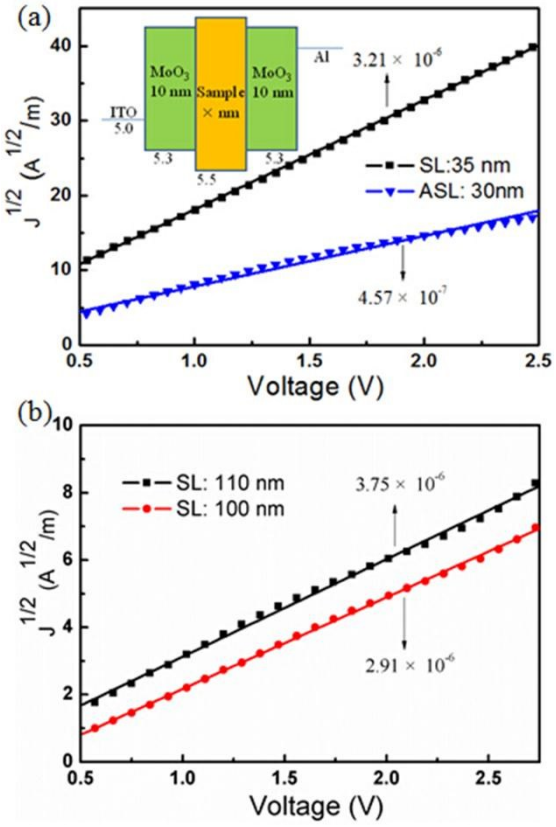

Figure 2. (a) The J-V curves of hole-only devices with SCLC fitting from SL and ASL (the structure of hole-only devices inserted in the picture). (b) The J-V curves of hole-only de-vices with SCLC fitting from SL.

The results of Mw distribution of SL and ASL were listed in Table S1. The Mw of ASL (Mw=1.53×10^5 Da, Mw/Mn=4.00) achieved a factor of 30-fold of SL (Mw=5.5×10^3 Da, Mw/Mn=2.12). To characterize the effect of $C_6H_{12}Br_2$ on the structure of SL, functional groups including phenolic hydroxyl groups and sulfonic groups were investigated. As shown in Table S1, Mw of ASL increased significantly accompanied by a remarkable decrease of phenolic hydroxyl group contents from 1.58 mmol/g to 0.11 mmol/g. It suggested that polymerization occurs on the position of phenol hydroxyl groups successfully. The content of sulfonic group of ASL decreased slightly with increasing Mw. To elucidate the chemical structure of ASL, FT-IR spectra of SL and ASL was conducted as shown in Figure S2. The intensity of bands at 2938 cm^{-1} and 2860 cm^{-1} corresponding to methylene stretching vibrations from alky chain increased significantly. The intensity of band at 1042 cm^{-1} corresponding to ether bond stretching vibration also

increased obviously, which further supported the efficient substitutions of aliphatic chains on the phenolic groups of SL. The samples were also subjected to ^{1}H-NMR analysis (Figure S3), the signal intensity between 0.5 and 2.0 ppm exhibited significant increase which was ascribed to aliphatic chain -C_6H_{12}- groups and was consistent with the IR results. Therefore, we proposed the reaction mechanism from AL to ASL as shown in Figure S1. AL was sulfomethylated to obtain SL, and then SL was polymerized with $C_6H_{12}Br_2$ to prepare supramolecular ASL polymer.

In order to make an quantitative evaluation on the different hole transport properties of the SL and ASL materials, their hole mobilities were measured by testing J-V characteristics of the hole-only devices with the device structure of ITO/MoO_3/Sample/MoO_3/Al as shown in Figure 2a. As a wide band gap semiconductor, MoO_3 is used to assist the holes transport to ITO anode and block the electrons injected from Al cathode at the same time. The observed dark current-voltage curves were then fitted by using the space-charge-limited current (SCLC) model, which is described by the equation as following:

$$J=(9/8)\varepsilon_r\varepsilon_0\mu(V^2/d^3)$$

In the equation above, ε_0 is the dielectric permittivity of free space, ε_r is the relative permittivity of the sample, μ is the mobility, and d is the thickness of sample. As shown in Figure 2, the hole mobility value was obtained by SCLC equation with the detailed data listed in Table 1.

Table 1. The hole mobilities of samples from SL and ASLs.

Samples	Thickness (L) (nm)	Slope (ρ)	Hole-mobility ($cm^2\ V^{-1}\ s^{-1}$)
SL	110	2.90	3.75×10^{-6}
SL	100	2.95	2.91×10^{-6}
SL	35	14.96	3.21×10^{-6}
ASL	30	6.46	4.57×10^{-7}

As can be seen from Figure 2a and Table 1, the hole mobility of 3.21×10^{-6} $cm^2\ V^{-1}\ s^{-1}$, achieved from sample SL, is nearly one order of magnitude higher than ASL. The result indicates that the SL and ASL are potential water soluble organic semiconductor with hole transporting properties. SL with more phenolic group content, has higher hole mobility than ASL with less phenolic group content, which suggested that phenolic group is conducive to the hole transporting property. In our study, SL with different thickness was also investigated as shown in Figure 2b, and the results were listed in Table 1. We can find that the hole mobilities of SL are all higher than that of ASL with different thickness. The maximum value of hole mobility achieved to 3.75×10^{-6} $cm^2\ V^{-1}\ s^{-1}$ from SL.

Base on the hole transporting properties of SL and ASL above, SL and ASL are potential organic semiconductor with hole transporting properties, especially for SL. Therefore, the electron transfer properties of SL and ASL were also studied in our work, including electrochemical property and electron spin resonance (ESR), as shown in Figure 3.

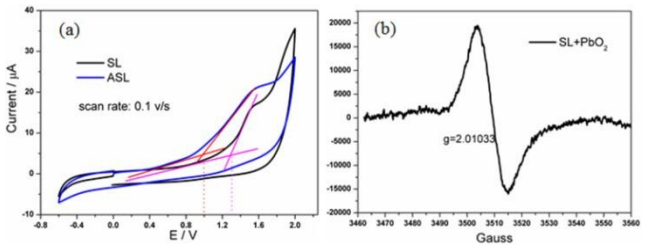

Figure 3. (a) Cyclic voltammogram curves of SL and ASL films in 0.1 M Bu_4NPF_6 DCM solution. (b) ESR spectrum of SL treated with PbO_2.

From the above results, the hole mobility of SL is higher than that of ASL, the oxidative activity of SL and ASL were also investigated. Cyclic voltammogram (CV) and Electron spin resonance (ESR) were applied to study the oxidative activity of samples. The cyclic voltammogram of samples in 0.1 M Bu_4NPF_6 (in dichloromethane) solution was used to investigate the electrochemical behaviour of SL and ASL as shown in Figure 3a. Two irreversible oxidation peaks at 1.0 V and 1.3 V were observed at the ASL and SL modified electrode, respectively. SL has relatively high oxidation potential at 1.3 V as the reported work.[45] The oxidation process of SL and ASL was also studied by ESR and obvious ESR signal of oxidized state of SL was observed in Figure 3b, which indicated that stable radicals were formed after the reaction of SL with PbO_2. SL was proposed to be oxidized to form resonance structure as proposed in Figure 1b during CV test. In contrast, ASL showed none of ESR signals at different concentrations and temperature including 100 K.

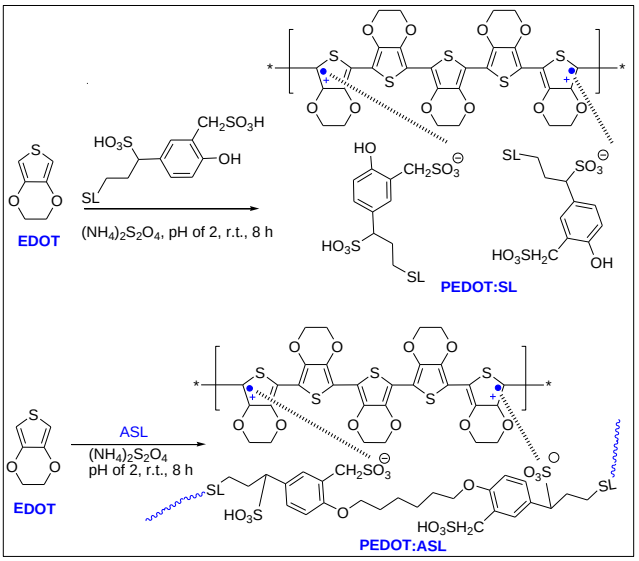

Figure 4. Proposed schematic for the polymerization of EDOT in the presence of SL (up) and ASL (down) polyelectrolyte templates.

On the basis of the above results, we can find that ASL with few phenolic group contents, which was obtained from alkyl chain cross-linked lignosulfonate, has lower hole mobility than SL with more phenolic group contents. Moreover, SL was also easy to aggregate and to be oxidized. In order to provide evidence to illustrate our proposal on the hole transport property of lignosulfonate, a series of water soluble and solution-processable PEDOT:SL and PEDOT:ASL were prepared by oxidation of EDOT dispersed in lignosulfonate. SL and ASL, as dispersant and template, were applied to be dopants in conductive polymer PEDOT, and the schematic for the polymerization of EDOT in the presence of SL and ASL templates was proposed as shown in Figure 4. The preparation of PEDOT:SL and PEDOT:ASL films were applied as hole transport layer in polymer solar cells devices, and PEDOT:PSS-4083 was also tested for the comparison.

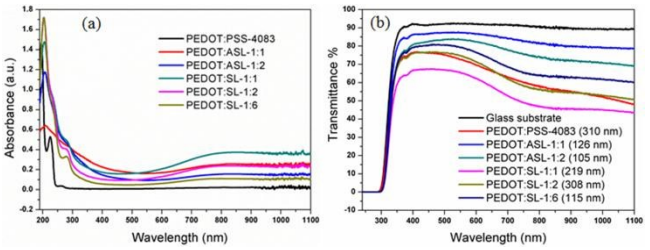

Figure 5. (a) UV-vis absorption spectra of PEDOT:PSS, PEDOT:ASL and PEDOT:SL with different mass ratio. (b) Transmittance of PEDOT:PSS film, PEDOT:ASL films and PEDOT:SL films with different mass ratio.

The UV-vis absorption spectra of PEDOT:SL and PEDOT:ASL aqueous dispersion were measured as shown in Figure 5a. The absorption bands at 280 nm originate from the aromatic rings of SL and ASL. All of UV spectra including PEDOT:PSS, PEDOT:SL and PEDOT:ASL aqueous dispersion showed the presence of a biopolaron absorption band at 800 nm, which was ascribed to the π-π transition in the PEDOT polymer chain.[46] In the meantime, the broad absorption from 600 to 900 nm was also detected in all PEDOT:SL and PEDOT:ASL aqueous dispersion. The transmittance spectra of PEDOT:SL and PEDOT:ASL films were shown in Figure 5b. The results indicated that the transmittance of the films was determined by both of the content of dopant and film thickness. The broad peak from 600 to 900 nm decreased compared with blank glass substrate in all PEDOT:SL and PEDOT:ASL films, which is consistent with the UV results.

To further study the structure of PEDOT:SL and PEDOT:ASL, the FT-IR spectra of EDOT, PEDOT:ASL-1:2 and PEDOT:SL-1:1 were showed in Figure 6. Compared with EDOT monomer, the strong band ascribed to the C-H bending mode at 892 cm^{-1} and the C-H vibration band at 2985 cm^{-1} and 3125 cm^{-1} all disappeared in the PEDOT:ASL and PEDOT:SL polymer spectra, demonstrating the formation of PEDOT chains with α, α'-coupling. Moreover, vibrations at 1480cm^{-1} and 1360cm^{-1} were attributed to the stretching modes of C=C and C-C in the thiophene ring, and the stretching vibration modes of the C-S

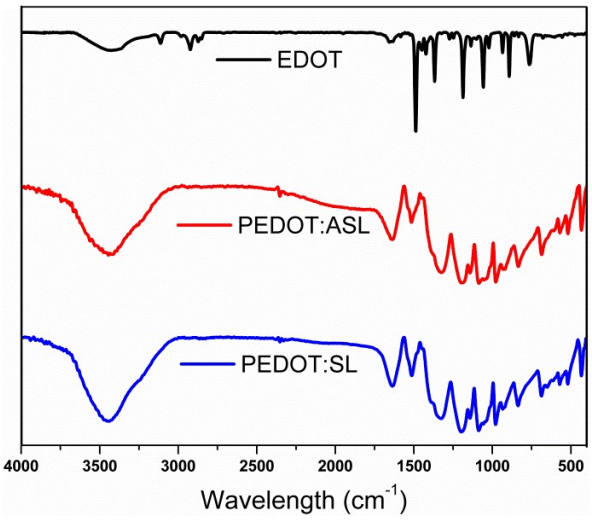

Figure 6. FT-IR spectra of EDOT monomer, PEDOT:ASL and PEDOT:SL.

bond in the thiophene ring can be observed at 935 cm^{-1} and 762 cm^{-1}. The adsorption peak at 1188 cm^{-1} and 620 cm^{-1} are attributed to the stretching modes of S=O bond of sulfonic groups. These show that PEDOT:SL and PEDOT:ASL have been prepared successfully.

The conductivities of PEDOT:PSS film, PEDOT:SL films and PEDOT:ASL films are shown in Table S2. The conductivities of PEDOT:SL with different proportion are close to that of PEDOT:PSS-4083, and the conductivity of PEDOT:SL-1:1 film (0.05 S/cm) is a litter higher than that of PEDOT:PSS-4083 film (0.02 S/cm). The sheet resistance of the films formed with PEDOT:ASL is too large to test.

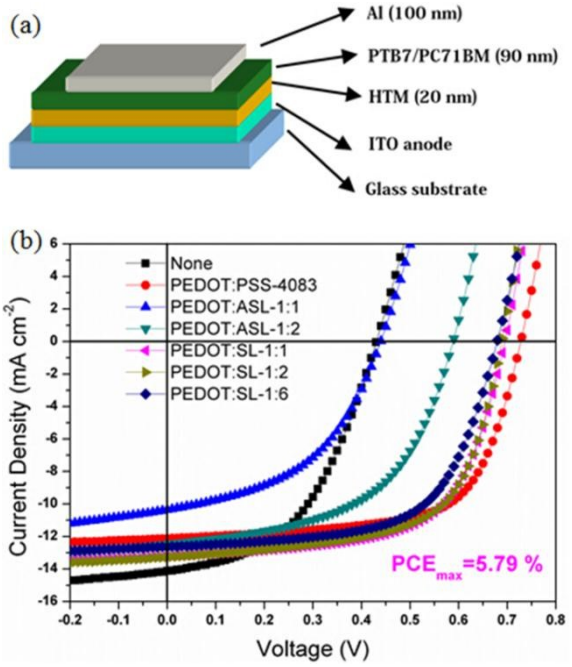

Figure 7. (a) Device architecture of the polymer solar cell (PSC). (b) J-V curves of PSCs with PEDOT only, PEDOT:PSS, PEDOT:LS and PEDOT:ASL with different mass ratio in devices of ITO/HTM/PTB7:PC_{71}BM/Al.

In order to evaluate the hole transport performance of PEDOT:SL film, PSCs with device structure ITO/HTM/PTB7: $PC_{71}BM$/Al were fabricated, in which water spin-coated PEDOT:SL and PEDOT:ASL were applied as HTM, respectively. Using PEDOT:PSS-4083 film as anode modifier, PSCs with the same devices structure were also prepared as control device for the comparison. The detailed device architecture and current density (J)-voltage (V) curves of the PSCs with different HTMs are shown in Figure 7. The power conversion efficiency (PCE), short-circuit current density (J_{SC}), open-circuit voltage (V_{OC}) and fill factor (FF) of the PSCs are given in Table 2. The PCE of the PSCs in a conventional device structure ITO/PEDOT:PSS/PTB7: $PC_{71}BM$/Al was 4.28 or 4.50% as the literatures reported[47,48] shown in Table 2. In our work, PEDOT only showed a bad PCE of 2.91% with a FF of 48.04%. The device with PEDOT:PSS modified anode showed a J_{SC} of 12.11, V_{OC} of 0.73 and PCE of 5.80% with a FF of 65.57%, which was relatively higher than the literatures reported. When the mass ratios of PEDOT:SL were 1:1, 1:2 and 1:6, respectively, the PCEs of device with PEDOT:SL were 5.79%, 5.76% and 5.33%, respectively, which were all very close to that of PEDOT:PSS-4083. However, PEDOT:ASL with different mass ratio exhibited relatively bad PCEs shown in Table 2. When the mass ratio of PEDOT:ASL was 1:1, the PCE of device was 2.14% which was lower than that of device using PEDOT-only anode, when PEDOT:ASL-1:2 was applied, a PCE of 3.93% with J_{SC} of 12.47 mA cm^{-2}, V_{OC} of 0.59 V and FF of 53.39% was obtained. It is noteworthy that PEDOT:SL with different mass ratio has the close performance which suggested the dependence of SL as dopant in conductive PEDOT polymer is not strong. The results indicates that SL has positive effect on the hole injection/transport properties. It encourages us to study its potential in the future. We proposed the possible mechanism based the following two aspects.

Table 2. Photovoltaic Performances of PSCs with PEDOT:PSS, PEDOT:ASL and PEDOT:SL with different proportion in devices of ITO/HTM/PTB7:$PC_{71}BM$/Al.

anode	pH	V_{OC}(V)	J_{SC}(ma cm^{-2})	FF(%)	PCE(%)
Reference[47]	—	0.72	12.77	46.40	4.28
Reference[48]	—	0.62	14.58	50.00	4.50
None	—	0.43	14.12	48.04	2.91
PEDOT:PSS	1.9	0.73	12.11	65.57	5.80
PEDOT:ASL-1:1	3.5	0.44	10.34	47.01	2.14
PEDOT:ASL-1:2	3.7	0.59	12.47	53.39	3.93
PEDOT:SL-1:1	3.6	0.70	13.22	62.60	5.79
PEDOT:SL-1:2	3.8	0.69	13.27	62.96	5.76
PEDOT:SL-1:6	3.9	0.68	12.64	62.03	5.33

First of all, in our work, alkyl chain was designed and introduced in phenolic group of SL to obtain high molecular weight lignosulfonate ASL, we found that hole mobility of ASL was lower than SL which suggested that phenolic group content could affect the hole transporting property. Therefore, SL could be applied to be dopant and template in conductive polymer PEDOT on the basis of the hole mobility and electron transfer property of SL, and exhibited better power conversion efficiency than ASL.

On the other hand, the aggregation behavior also affects the hole transporting property of conductive PEDOT. Therefore, the surface morphologies of PEDOT:PSS, PEDOT:ASL and PEDOT:SL with different mass ratio were observed by AFM as shown in Figure 6a-f. There is significant difference between them. The surface of PEDOT:PSS-4083 was quite smooth (Figure 8a). In comparison, the surfaces of PEDOT:SL and PEDOT:ASL were unique and different from that of PEDOT:PSS, which was consisted of many compact nanoaggregates (Figure 8b-f). We also found that the surface and the size of the nanoaggregates between them were different. The size of the aggregates from PEDOT:SL was relatively smaller than that from PEDOT:ASL, and the aggregates from PEDOT:SL was more compact than that from PEDOT:ASL, which both contributed to the unexpected hole transport of PEDOT:SL film. The AFM images of the film after heating (120 ℃ for 20 min) were also shown in Figure S4 and Figure 8g-i. The crystalline characteristic of samples all decreased, however, the obvious nanoaggregate after thermal annealing from PEDOT:SL might facilitate charge transport of PEDOT:SL polymers in film as shown in Figure 8g-i.

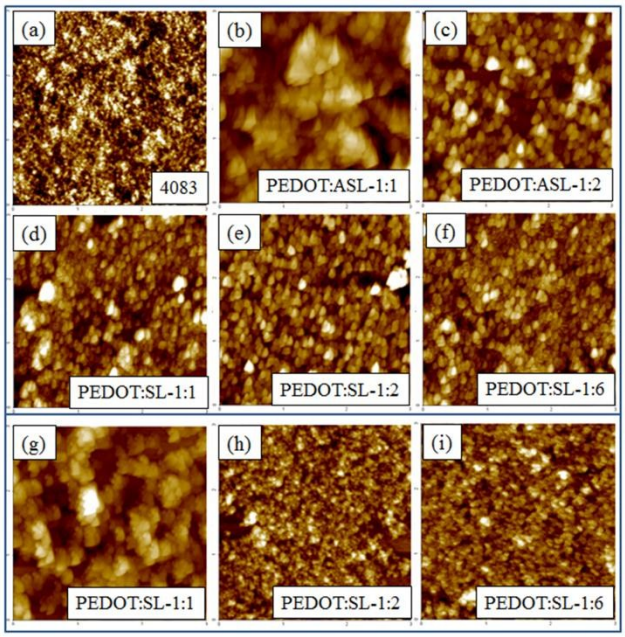

Figure 8. AFM images of PEDOT:PSS (Baytron PVPAI 4083) film (a) , PEDOT:ASL film (b,c) and PEDOT:SL film (d-f). (g-i) the film after heating (120 ℃ for 20 min) from PEDOT:SL with different mass ratio. The size of the images is 3 μm×3 μm.

PEDOT:SL showed promising performance as hole-transport material in polymer solar cells (PSCs), which is comparable with that of conversional PEDOT:PSS. As we know that lignosulfonate is totally amorphous and complex, however, poly(styrenesulfonate) (PSS) has regular structure with crystallizability. In principle, comparing with PSS, lignosulfonate will show worse hole transport property as dopant for PEDOT. In contrast, we found PEDOT:SL showed comparable performance with that of PEDOT:PSS. This also confirmed our proposal and results on the hole transport

property of lignosulfonate. It is worth mentioning that the new HTMs including their properties have reproducitivity with different lignosulfonate. Our results provide a promising scaffold and concept for the design and feasible synthesis of HTMs based on the interconversion between phenol and benzoquinone for organic electronics in future.

Experimental

Materials

Alkali lignin (AL) separated from the pulping black liquor was supplied by Shuntai Co. Ltd. (Shuntai, Hunan, China). 1,6-Dibromohexane ($C_6H_{12}Br_2$) was supplied by Energy Chemical Co. Ltd. (Shanghai, China) with a purity of 97%. All other chemicals were of analytical grade, including NaOH, Na_2SO_3, KI, hexane, ethanol (EtOH), formaldehyde (CH_2O) of 37%.

Modification of alkali lignin

AL (10 g) was dissolved in 50 mL of H_2O at pH of 12. The reaction was started by slow addition of formaldehyde (2.1 g) at 70 ℃ for 20 min, and subsequent addition of sodium sulfite (4.0 g) at 95 ℃. After the reaction was kept for 3 hours, the reaction liquid was added a certain amount of $C_6H_{12}Br_2$ reagent, 5.0 g of NaOH and trace amount of KI (0.1 g) at 75 ℃, respectively. The ratios of m (AL): m ($C_6H_{12}Br_2$) was 1.0:0.65. The polymerization was stopped after reflux at 75 ℃ for 10 hours. The sample was then extracted with hexane to remove the excessive $C_6H_{12}Br_2$ and the polymer in aqueous solution was filtered. The filtrates were purified with dialysis. The purified product was then freeze-dried to obtain yellow-brown solid powder sample.

Characterization

The Mw measurement was conducted by aqueous gel permeation chromatography and the UV absorption at 280 nm was monitored with a Waters 2487 UV detector (Waters Co, Milford, MA, USA). Polystyrene sulfonate was used as calibration standard. A 0.10 M $NaNO_3$ solution (pH 8.0) was used as mobile phase (0.50 mL/min). Samples were dissolved and diluted into 0.3 wt% using double-distilled water and filtered by a 0.22 μm filter.

The phenolic hydroxyl group (-OH) content of samples was determined by FC method. The sulfonic group ($-SO_3H$) content of SL and ASL was measured by automatic potentiometric titrator (Type 809 Titrando, Metrohm Corp., Switzerland).

Fourier transform infrared spectrometry of Auto system XL/I-series/Spectrum2000 (Thermo Nicolet Co., Madison, WI, USA) was used for infrared spectrum analysis and recorded between 4000 and 400 cm^{-1}. The measurement method was potassium bromide pressed-disk technique.

The ^{1}H-NMR spectra of SL and ASL were recorded with 30 mg of each sample dissolved in 0.5 mL of deuterated dimethylsulfoxide (DMSO-d_6) using DRX-400 spectrometer (Bruker Co., Ettlingen, Germany).

The hole mobility of samples was measured using space-charge-limited current (SCLC) method by testing J-V characteristics of hole-only device structure: ITO/MoO_3 (10 nm)/Sample/MoO_3 (10 nm)/Al (100 nm). The film of sample was spin-coated with concentration of 80 mg mL^{-1} and the solvent of sample is deionized water.

Cyclic voltammetry measurement was conducted as follows: a glassy carbon electrode was first polished carefully with alumina powder to a mirror finish surface and rinsed with distilled water repetitively. Sample solution was prepared by dissolving 10 mg sample in 1 mL distilled water. Then SL and ASL polymer films were deposited at the surface of the clean glassy carbon electrode. The resulting electrode was immersed in 0.1 M Bu_4NPF_6 DCM solutions, and was stabilized in 0.1 M Bu_4NPF_6 DCM solutions by scanning the potential between -0.6 and +2.0 V at a scan rate of 100 mV/s.

ESR spectra were recorded on a JEOL model JES-FA200 spectrometer (JEOL, Japan) operating at 9.058 GHz with a 100 kHz modulation frequency.

Atomic force microscope (AFM) images were observed using Park XE-100 instrument by tapping mode. The AFM samples were prepared by spinning the sample solution on the ITO conductive substrate.

Preparation and characterization of PEDOT:SL and PEDOT:ASL

A proposed schematic for the polymerization of EDOT in the presence of SL and ASL dispersants is shown in Figure 4. The procedure was prepared as follows. SL or ASL sample with different mass was dissolved in 200 mL of distilled water, then 1 g EDOT monomer was added with slow stirring speed for 10 min and the pH value of the solution was adjusted to 2. To the mixed solution, 1.93 g of oxidant ammonium persulfate (APS) solution was added slowly under high speed stirring. The reaction was kept at room temperature for 24 hours, and dialyzed to remove inorganic salt. The dialysis product was used for detection through ultrasonication for 10 min. PEDOT:PSS (Baytron PVPAI 4083) was used for the comparison. The UV-vis absorption spectra of PEDOT:PSS (Baytron PVPAI 4083), PEDOT:SL and PEDOT:ASL aqueous dispersion were measured using Shimadzu UV-3600 spectrophotometer (Japan). The transmittance spectra of PEDOT:PSS-4083 film, PEDOT:SL films and PEDOT:ASL films were tested using Shimadzu UV-2600 spectrophotometer (Japan). The FT-IR spectra of PEDOT:ASL and PEDOT:SL polymer were also measured. The sheet resistance of PEDOT:PSS film, PEDOT:ASL films and PEDOT:SL films was tested by KDY-1 four point probes resistivity/resistance measurement system, and the film thickness of the film samples was tested using the step profiler (Dektak 150, Veeco, USA).

Fabrication and characterization of OPVs

ITO-coated glass substrates were cleaned by sonication in acetone, detergent, deionized water, and isopropyl alcohol and dried in a nitrogen stream, followed by an oxygen plasma treatment. In order to fabricate photovoltaic devices, a thin hole-transportation layer (ca. 40 nm) of PEDOT:sample (filtered at 0.45 μm) was spin-cast on the pre-cleaned ITO-coated glass substrates and baked at 120 ℃ for 20 min under ambient conditions. The active layer PTB7:PC71BM (10:15 mg/mL) was prepared by spin-casting chlorobenzene solution with the addition of a small amount of DIO (CB: DIO = 100:3, V/V) at 1500 rpm for 30 s in dry box. The thickness of the PTB7:PC71BM layer was about 100 nm. 4 h later, methanol

was spin-coated on the active layer at 2000 rpm for 30 s. The Al electrode were thermally deposited for 100 nm through a mask in vacuum (<5 × 10^{-4} Pa). All steps except processing of HTMs were performed in the glove box. The effective device area was about 0.16 cm^2. The current density–voltage (J–V) characteristics were measured using a Keithley 2400 source meter. The photovoltaic devices were characterized using a calibrated AM1.5 G solar simulator (Oriel model 91192), under light intensity of 100 mW/cm^2.

Conclusions

To summarize, the hole-transporting properties of water soluble lignosulfonate and alkyl chain cross-linked lignosulfonate polymers were studied by hole-only devices for the first time. The underlying mechanism was the electron transfer process during oxidation of electron-rich phenol derivative structure and serious aggregation properties of lignosulfonate. The unexpected hole mobility provide a novel prospective for application of lignosulfonate as a potential polymeric p-type semiconductor. A water soluble and solution-processable PEDOT:SL prepared by oxidation of EDOT dispersed in SL showed promising performance as hole-transport material in polyer solar cells, which is comparable with that of conversional PEDOT:PSS. In addition, PEDOT:SL might show potential for application in various of fields including PEDOT:PSS-based Hybrid Solar Cells[49-53].Our results provide a novel concept for the application of biradicals containing polyaromatic hydrocarbons[54-56] and provide a promising scaffold for the design and feasible synthesis of HTMs based on the interconversion between phenol and benzoquinone for organic electronics in future.

Acknowledgements

The authors would like to acknowledge the financial support of National Natural Science Foundation of China (21402054, 21436004), National Basic Research Program of China 973 (2012CB215302), International S&T Cooperation Program of China (2013DFA41670).

Notes and references

1 Q. L. Huang, G. A. Evmenenko, P. Dutta, P. Lee, N. R. Armstrong and T. J. Marks, *J. Am. Chem. Soc.,* 2005, **127**, 10227-10242.
2 P. Kundu, K. R. J. Thomas, J. T. Lin, Y. T. Tao and C. H. Chien, *Adv. Funct. Mater.,* 2003, **13**, 445-452.
3 V. I. Adamovich, S. R. Cordero, P. I. Djurovich, A. Tamayo, M. E. Thompson, B. W. D'Andrade and S. R. Forrest, *Org. Electron.,* 2003, **4**, 77-87.
4 D. Y. Kondakov, J. R. Sandifer, C. W. Tang and R. H. Young, *J. Appl. Phys.,* 2003, **93**, 1108-1119.
5 D. N. Congreve, J. Y. Lee, N. J. Thompson, E. Hontz, S. R. Yost, P. D. Reusswig, M. E. Bahlke, S. Reineke, T. Van Voorhis and M. A. Baldo, *Science,* 2013, **340**, 334-337.
6 P. Peumans, S. Uchida and S. R. Forrest, Nature, 2003, **425**, 158-162.
7 G. Teran-Escobar, J. Pampel, J. M. Caicedo and M. Lira-Cantu, *Energy Environ. Sci.,* 2013, **6**, 3088-3098.
8 S. Berny, L. Tortech, M. Veber and D. Fichou, *ACS Appl. Mater. Inter.,* 2010, **2**, 3059-3068.
9 A. Facchetti, *Mater. Today,* 2007, **10**, 28-37.
10 X. Y. Cheng, Y. Y. Noh, J. P. Wang, M. Tello, J. Frisch, R. P. Blum, A. Vollmer, J. P. Rabe, N. Koch, H. Sirringhaus, *Adv. Funct. Mater.,* 2009, **19**, 2407-2415.
11 S. Y. Shao, J. Liu, J. Bergqvist, S. W. Shi, C. Veit, U. Wurfel, Z. Y. Xie and F. L. Zhang, *Adv. Energy Mater.,* 2013, **3**, 349-355.
12 L. Chen, C. Xie and Y. W. Chen, *Adv. Funct. Mater.,* 2014, **24**, 3986-3995.
13 Y. Sun, S. C. Chien, H. L. Yip, Y. Zhang, K. S. Chen, D. F. Zeigler, F. C. Chen, B. P. Lin and A. K. Y. Jen, *Chem. Mater.,* 2011, **23**, 5006-5015.
14 T. M. Brown, J. S. Kim, R. H. Friend, F. Cacialli, R. Daik and W. J. Feast, *Appl. Phys. Lett.,* 1999, **75**, 1679-1681.
15 M. Vosgueritchian, D. J. Lipomi and Z. A. Bao, *Adv. Funct. Mater.,* 2012, **22**, 421-428.
16 H. L. Yip and A. K. Y. Jen, *Energ. Environ. Sci.,* 2012, **5**, 5994-6011.
17 S. K. Hau, H. L. Yip, N. S. Baek, J. Y. Zou, K. O'Malle and A. K. Y. Jen, *Appl. Phys. Lett.,* 2008, **92**, 253301-253303.
18 K. Kawano, R. Pacios, D. Poplavskyy, J. Nelson, D. D. C. Bradley and J. R. Durrant, *Sol. Energy Mater. Sol. Cells,* 2006, **90**, 3520-3530.
19 A. W. Hains, Z. Q. Liang, M. A. Woodhouse and B. A. Gregg, *Chem. Rev.,* 2010, **110**, 6689-673.
20 C. E. Tsai, M. H. Liao, Y. L. Chen, S. W. Cheng, Y. Y. Lai, Y. J. Cheng and C. S. Hsu, *J. Mater. Chem. A.,* 2015, **3**, 6158-6165.
21 Y. Wei, P. J. Liu, R. H. Lee and C. P. Chen, *RSC Adv.,* 2015, **5**, 7897-7904.
22 X. D. Li, X. H. Liu, X. Y. Wang, L. X. Zhao, T. G. Jiu and J. F. Fang, *J. Mater. Chem. A.,* 2015, **3**, 15024-15029.
23 C. K. Song, A. C. White, L. Zeng, B. J. Leever, M. D. Clark, J. D. Emery, S. J Lou, A. Timalsina, L. X. Chen, M. J. Bedzyk and T. J. Marks, *ACS Appl. Mater. Inter.,* 2013, **5**, 9224-9240.
24 E. L. Ratcliff, A. Garcia, S. A. Paniagua, S. R. Cowan, A. J. Giordano, D. S. Ginley, S. R. Marder, J. J. Berry and D. C. Olson, *Adv. Energy Mater.,* 2013, **3**, 647-656.
25 Z. W. Wu, S. Bai, J. Xiang, Z. C. Yuan, Y. G. Yang, W. Cui, X. Y. Gao, Z. Liu, Y. Z. Jin and B. Q. Sun, *Nanoscale,* 2014, **6**, 10505-10510.
26 J. H. Kim, P. W. Liang, S. T. Williams, N. Cho, C. C. Chueh, M. S. Glaz, D. S. Ginger and A. K. Y. Jen, *Adv. Mater.,* 2015, **27**, 695-701.
27 W. Chang, D. N. Congreve, E. Hontz, M. E. Bahlke, D. P. McMahon, S. Reineke, T. C. Wu, V. Bulović, T. Van Voorhis and M. A. Baldo, *Nat. Commun.,* 2015, **6**.
28 C. W. Tang, S. A. VanSlyke and C. H. Chen, *J. Appl. Phys.,* 1989, **65**, 3610-3616.
29 Z. Q. Gao, C. S. Lee, I. Bello and S. T. Lee, *Synthetic Met.,* 2000, **111**, 39-42.
30 D. Alemu, H. Y. Wei, K. C. Ho and C. W. Chu, *Energ. Environ. Sci.,* 2012, **5**, 9662-9671.
31 S. J. Lee, A. B. Yusoff and J. Jang, *RSC Adv.,* 2014, **4**, 20242-20246.
32 S. Q. Xiao, L. Chen, L. C. Tan, L. Q. Huang, F. Y. Wu and Y. W. Chen, *J. Phys. Chem. C.,* 2015, **119**, 1943-1952.
33 J. Meyer, S. Hamwi, M. Kroger, W. Kowalsky, T. Riedl and A. Kahn, *Adv. Mater.,* 2012, **24**, 5408-5427.
34 P. J. Low, M. A. J. Paterson, D. S. Yufit, J. A. K. Howard, J. C. Cherryman, D. R. Tackley, R. Brook and B. Brown, *J. Matter. Chem.,* 2005, **15**, 2304-2315.
35 X. J. Pan, J. F. Kadla, K. Ehara, N. Gilkes and J. N. Saddler, *J. Agr. Food Chem.,* 2006, **54**, 5806-5813.
36 W. Boerjan, J. Ralph and M. Baucher, *Annu. Rev. Plant Biol.,* 2003, **54**, 519-546.
37 F. G. Calvo-Flores and J. A. Dobado, *Chemsuschem,* 2010, **3**, 1227-1235.

38 F. Chen and R. A. Dixon, *Nat. Biotechnol.,* 2007, **25**, 759-761.
39 J. Zakzeski, P. C. A. Bruijnincx, A. L. Jongerius and B. M. Weckhuysen, *Chem. Rev.,* 2010, **110**, 3552-3599.
40 C. P. Xu, R. A. D. Arancon, J. Labidi and R. Luque, *Chem. Soc. Rev.,* 2014, **39**, 1266-1290.
41 S. Laurichesse and L. Averous, *Prog. Polym. Sci.,* 2014, **39**, 1266-1290.
42 Y. Qian, X. Q. Qiu and S. P. Zhu, *Green Chem.,* 2015, **17**, 320-324.
43 Y. H. Deng, X. J. Feng, M. S. Zhou, Y. Qian, H. F. Yu and X. Q. Qiu, *Biomacromolecules,* 2011, **12**, 1116-1125.
44 N. L. Hong, Y. Li, W. M. Zeng, M. K. Zhang, X. W. Peng and X. Q. Qiu, *RSC Adv.,* 2015, **5**, 21588-21595.
45 X. H. Liu, L. Jiang, J. S. Li, L. Wang, Y. Yu, Q. Zhou, X. X. Lv, W. M. Gong, Y. Lu and J. Y. Wang, *J. Am. Chem. Soc.,* 2014, **136**, 13094-13097.
46 J. Ouyang, Q. F. Xu, C. W. Chu, Y. Yang, G. Li and J. Shinar, *Polymer,* 2004, **45**, 8443-8450.
47 M. V. Srinivasan, M. Ito, P. Kumar, K. Abhirami, N. Tsuda, J. Yamada, P. K. Shin and S. Ochiai, *Ind. Eng. Chem. Res.,* 2015, **54**, 181-187.
48 S. Guo, B. Y. Cao, W. J. Wang, J. F. Moulin and P. Muller-Buschbaum, *ACS Appl. Mater. Inter.,* 2015, **7**, 4641-4649.
49 J. P. Thomas, L. Y. Zhao, D. McGillivray and K. T. Leung, *J. Mater. Chem. A.,* 2014, **2**, 2383-2389.
50 J. P. Thomas, S. Srivastava, L. Y. Zhao, M. Abd-Ellah, D. McGillivray, J. S. Kang, M. A. Rahman, N. Moghimi, N. F. Heinig and K. T Leung, *ACS Appl. Mater. Inter.,* 2015, **7**, 7466-7470.
51 J. P. Thomas and K. T. Leung, *Adv. Funct. Mater.,* 2014, **24**, 4978-4985.
52 P. C. Yu, C. Y. Tsai, J. K. Chang, C. C. Lai, P. H. Chen, Y. C. Lai, P. T. Tsai, M. C. Li, H. T. Pan, Y. Y. Huang, C. I. Wu, Y. L. Chueh, S. W. Chen, C. H. Du, S. F. Horng and H. F. Meng, ACS Nano, 2013, 7, 10780-10787.
53 J. P. Thomas, L. Y Zhao, M. Abd-Ellah, N. F. Heinig and K. T. Leung, *Anal. Chem.,* 2013, **85**, 6840-6845.
54 Y. Li, W. K. Heng, B. S. Lee, N. Aratani, J. L. Zafra, N. Bao, R. Lee, Y. M. Sung, Z. Sun, K. W. Huang, R. D. Webster, J. T. L. Navarrete, D. Kim, A. Osuka, J. Casado, J. Ding and J. S. Wu, *J. Am. Chem. Soc.,* 2012, **134**, 14913–14922.
55 Z. B. Zeng, Y. M. Sung, N. N. Bao, D. Tan, R. Lee, J. L. Zafra, B. S. Lee, M. Ishida, J. Ding, J. T. L. Navarrete, Y. Li, W. D. Zeng, D. Kim, K. W. Huang, R. D. Webster, J. Casado and J. S. Wu, *J. Am. Chem. Soc.,* 2012, **134**, 14513-14525.
56 Z. B. Zeng, M. Ishida, J. L. Zafra, X. J. Zhu, Y. M. Sung, N. N. Bao, R. D. Webster, B. S. Lee, R. W. Li, W. D. Zeng, Y. Li, C. Y. Chi, J. T. L. Navarrete, J. Ding, J. Casado, D. Kim and J. S. Wu, *J. Am. Chem. Soc.,* 2013, **135**, 6363–6371.

Table of Contents (TOC)

As a hole transport material, PEDOT dispersed with lignosulfonate was prepared and showed promising performance in polymeric solar cells.